(2) E. W. Dempsey and R. S. Morison, *ibid.*, **135**, 293(1942a).
(3) *Ibid.*, **135**, 301(1942b).
(4) L. Angyan, E. Grastyan, and G. T. Sakhiulina, *Fed. Proc. (Trans. Suppl.)*, **23**, T264(1964).
(5) E. Grastyan, G. T. Sakhiulina, and L. Angyan, *Acta Physiol. Acad. Sci. Hung.*, **23**, 155(1963).
(6) E. Grastyan and L. Angyan, *Physiol. Behav.*, **2**, 5(1967).
(7) G. T. Sakhiulina and G. K. Merzhanova, *Electroenceph. Clin. Neurophysiol.*, **17**, 497(1964).
(8) J. Pecci-Saavedra, R. W. Doty, and H. B. Hunt, *ibid.*, **19**, 492(1965).
(9) E. F. Domino, *J. Pharmacol. Exp. Ther.*, **115**, 449(1955).
(10) F. Rinaldi and H. E. Himwich, *Dis. Nerv. Syst.*, **16**, 133(1955).
(11) E. K. Killam and K. F. Killam, *J. Pharmacol. Exp. Ther.*, **116**, 35(1956).
(12) M. Monnier and P. Krupp, *Schweiz. Med. Wochenschr.*, **89**, 430(1959).
(13) E. B. Sigg, *Can. Psychiat. Ass. J., Suppl.*, **4**, S75(1959).
(14) P. Crepax, E. Fadiga, and A. Volta, *Boll. Soc. Ital. Biol. Sper.*, **37**, 180(1961).
(15) H. H. Jasper and C. A. Ajmone-Marsan, "A Stereotaxic Atlas of the Diencephalon of the Cat," National Research Council of Canada, Ottawa, Canada, 1954.
(16) N. A. Buchwald, E. J. Wyers, B. A. Lauprecht, and G. Heuser, *Electroenceph. Clin. Neurophysiol.*, **13**, 531(1961).
(17) N. A. Buchwald and C. D. Hull, *Brain Res.*, **6**, 1(1967).
(18) S. Courvoisier, J. Fournel, R. Ducrot, M. Kolsky, and P. Koetschet, *Arch. Int. Pharmacodyn. Ther.*, **92**, 305(1953).
(19) D. R. Maxwell and H. T. Palmer, *Nature (London)*, **191**, 84(1961).
(20) L. T. Rutledge and R. W. Doty, *Amer. J. Physiol.*, **191**, 189(1957).
(21) J. E. Skinner, *Electroenceph. Clin. Neurophysiol.*, **31**, 197(1971).

ACKNOWLEDGMENTS AND ADDRESSES

Received November 1, 1974, from the *Department of Pharmacodynamics, Warner-Lambert Research Institute, Morris Plains, NJ 07950*

Accepted for publication February 24, 1975.

Adapted in part from a thesis submitted by B. Dubinsky to the University of Pittsburgh in partial fulfillment of the Doctor of Philosophy degree requirements.

Supported in part by the American Foundation for Pharmaceutical Education and by Public Health Service Grant FR 05455.

* Present address: School of Pharmacy, University of Maryland, Baltimore, MD 21201

‡ Present address: College of Pharmacy, University of Houston, Houston, TX 77004

ˣ To whom inquiries should be directed.

Nonsink Dissolution Rate Equations

MAHENDRA PATEL and J. T. CARSTENSEN ˣ

Abstract □ In spite of the fact that film theory is based on severe assumptions, it is shown to be a good working model. The Niebergall–Goyan equation, the Short–Sharkey–Rhodes equation, and the Pothisiri–Carstensen equation—all based on simple film theory—are shown to hold through 80–90% of the dissolution process for *p*-hydroxybenzoic acid and sodium chloride, both at values below and above the amount necessary to saturate the dissolution medium. Deviations are attributed to experimental difficulties and to improper definition of monodisperseness rather than to the assumptions made in the theory.

Keyphrases □ Nonsink dissolution of monodisperse powders—various rate equations examined □ Dissolution of monodisperse powders—various rate equations examined □ Powders, monodisperse—various nonsink dissolution rate equations examined

Dissolution of monodisperse powders has been studied and reported by several investigators. The intents of this study are to consolidate a variety of equations, to point out their shortcomings and strengths, and to show that film theory is a good working model.

BACKGROUND

The dissolution rate equations dealt with here are based on the Noyes–Whitney equation (1):

$$-dW/dt = kO(S - C) \qquad \text{(Eq. 1)}$$

where W is the weight remaining, k is the intrinsic dissolution rate constant, O is the surface area, S is the saturation concentration, and C is the concentration at time t.

The assumptions made are: *(a)* a film [the so-called Nernst–Brunner layer (2–4)] surrounds each particle; *(b)* the film need not be hydrodynamically stagnant but behaves so that there is a linear concentration gradient in it; and *(c)* the concentration gradient imparts a concentration, C, at the boundary between the film and the bulk solution. The thickness of this boundary is assumed not to change during dissolution; *i.e.*, it is assumed to be independent of particle size. Niebergall *et al.* (5) studied this point, but it will not be discussed in this report.

Another assumption is that the particles are isotropic and isometric, although Carstensen and Patel (6) showed that this condition need not be a prerequisite. The Ostwald–Freundlich effect (7, 8), where a smaller particle is more soluble than a larger particle, is also neglected.

A dissolution rate equation for monodisperse powders was first suggested by Wilhelm *et al.* (9); they employed graphical integration to solve exact dissolution rate equations. Hixson and Crowell (10) arrived at the cube root law for dissolution of monodisperse powders under sink conditions (*i.e.*, when $C \ll S$):

$$W_o^{1/3} - W^{1/3} = \frac{W_o^{1/3} 2kS}{\rho d} t \qquad \text{(Eq. 2)}$$

where d is the diameter of the particle (assumed spherical), and ρ is the particle density. For Fick's law (11) to apply to film theory, it is required that:

$$k = D/h \qquad \text{(Eq. 3)}$$

where D is the diffusion coefficient of the solute in solution, and h is the thickness of the Nernst–Brunner layer. Since D can be determined experimentally or obtained by the Stokes–Einstein equation (12) or the Wilke equation (13), an estimate of h can be made from dissolution rate studies.

Niebergall and Goyan (14) extended the Hixson–Crowell equation to the situation where the amount studied (W_o) equals exactly

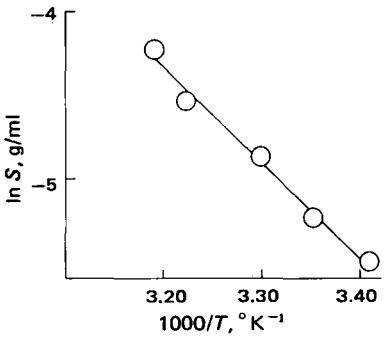

Figure 1—*Temperature dependence of the solubility of* p-*hydroxybenzoic acid.*

the amount needed to saturate the solution (W_s). As shown in the *Appendix*, they found the negative two-thirds law as expressed in Eq. 4:

$$W^{-2/3} - W_o^{-2/3} = \beta t \qquad \text{(Eq. 4)}$$

where the proportionality constant β is given by: $\beta = kN^{1/3}\Gamma/V$, in which N is the number of particles and Γ is a shape factor given by: $\Gamma = [6\sqrt{\pi}/\rho]^{2/3}$. Niebergall and Goyan (14), employing salicylamide and benzoic acid as test substances, showed Eq. 4 to hold but only to about 30% of saturation.

Short *et al.* (15) solved the dissolution rate equation under nonsink conditions, where W_s is different from W_o. The correct form of their equation with the nomenclature used here is:

$$\psi(W) = -[(k\sqrt[3]{N})(\Gamma/V)]t + \psi(W_o) \qquad \text{(Eq. 5)}$$

where:

$$\psi(W) = 0.5F^{-2}\{\ln[(u+F)^2/(F^2 - uF + u^2)]\} + \sqrt{3}F^{-2}\arctan[(2u - F)/(F\sqrt{3})] \qquad \text{(Eq. 6)}$$

and where $F^3 = W_s - W_o$ and $W = u^3$. The derivation of Eq. 5 is shown in the *Appendix*. Short *et al.* (15) tested the equation on the dissolution of hydrocortisone and found it *not* to hold.

Pothisiri and Carstensen (16) developed a similar equation under nonsink conditions; the correct form of their equation with the nomenclature used here is[1]:

$$\psi(r) = \psi(r_o) - \frac{k}{\rho}t \qquad \text{(Eq. 7)}$$

where:

$$\psi(r) = \frac{q}{6\beta}\ln\left[\frac{(r+q)^2}{(r^2 - qr + q^2)}\right] + \frac{q}{\beta\sqrt{3}}\arctan\left[\frac{2r - q}{q\sqrt{3}}\right] \qquad \text{(Eq. 8)}$$

where r is the "radius" of the particle; $\alpha = N\rho 4\pi/(3V)$, where V is the volume of the dissolving medium; $\beta = S - (W_o/V)$; and $q^3 = \beta/\alpha$. All derived equations are based on film theory. Pothisiri and Carstensen (16) showed Eq. 8 to hold up to 65% of saturation. Although simple film theory should fail on many counts (17, 18), it, amazingly, gives excellent correlation with experimental values.

EXPERIMENTAL

p-Hydroxybenzoic acid dissolution was tested in a 1000-ml jacketed beaker[2]. The *p*-hydroxybenzoic acid was recrystallized in a nonisothermal fashion (6) from alcohol USP, air dried, and sieved through a nest of sieves. The fraction retained by a 60-mesh screen and passing a 40-mesh screen was used in most experiments. One particular experiment was conducted with a 16–20-mesh cut; but unless otherwise stated, the experiments refer to the 40–60-mesh cut.

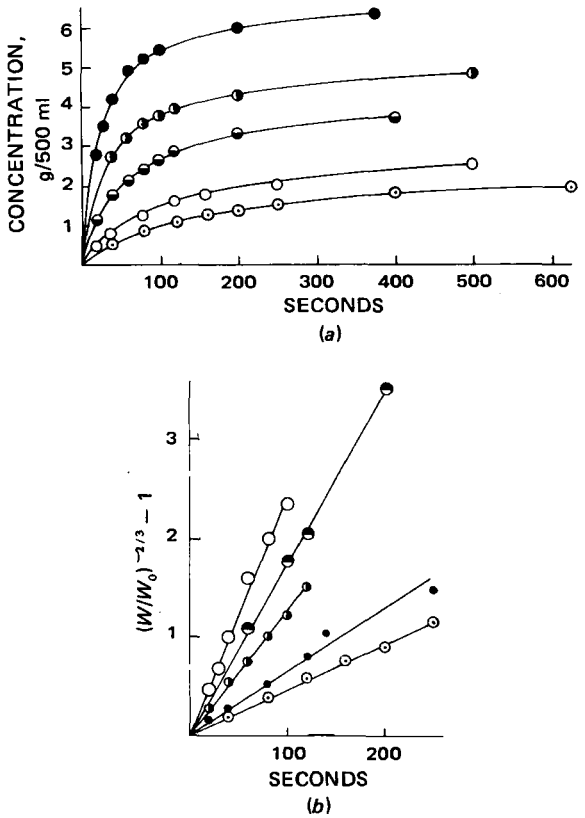

Figure 2—*(a) Concentration* versus *time profile for* p-*hydroxybenzoic acid at different temperatures in 0.1* N *HCl (initial weight* $W_o = W_s$*). Key: ⊙, 20°; ○, 25°; ⊖, 30°; ◑, 35°; and ●, 40°.* (b) *Plots of data from Fig. 2a plotted according to Eq. 4. Key: ⊙, 20°; ●, 25°; ◑, 30°; ⊖, 35°; and ○, 40°. The slopes of the lines are denoted* B.

Several batches were made in this fashion, and the various cuts were pooled to obtain adequate yields for the dissolution rate studies. The dimensions of the 1000-ml jacketed beaker were 8 cm in diameter and 18 cm in height; it was agitated by a Teflon-coated magnetic stirring bar, 8 mm in diameter and 36 mm in length, operating at 120 rpm. The jacket was connected with Tygon tubing *via a pump*[3] *to a thermostated bath, so the jacket temperature* could be maintained to ±0.3°. An amount of 0.1 *N* HCl slightly in excess of 500 ml was placed in a 500-ml volumetric flask, the flask was placed in the water bath, and the temperature was equilibrated.

The amount in excess of 500 ml was removed by pipet, and the 500 ml was transferred to the jacketed beaker. An excess of *p*-hydroxybenzoic acid (*i.e.*, an amount in excess of the solubility) was added to the solution, and the beaker was then covered with aluminum foil. The concentration of *p*-hydroxybenzoic acid in the supernate was determined from time to time; when a steady level had been reached (24 hr), the concentration was assumed to be the saturation concentration. The temperature of the contents was determined periodically and found to vary by less than 0.6° at the extremes, *i.e.*, ±0.3°. The experiment was carried out at 20, 25, 30, 35, and 40°. The assay method used was the spectrophotometric method described by Pothisiri and Carstensen (16). The solubility as a function of temperature is shown in Fig. 1.

The experiment was then repeated except that exactly the amount of *p*-hydroxybenzoic acid necessary to saturate the 500 ml of 0.1 *N* HCl at the test temperature (W_s) was added, and (approximately) 1-ml samples were removed through glass wool with a tared hypodermic syringe which was then weighed. The contents were transferred quantitatively to a volumetric flask, assayed, and

[1] The last fraction in Eq. 11 of the paper by Pothisiri and Carstensen (16) is inverted, and the equation should read as shown in Eq. 8 here. The solubility reported in Ref. 16 is higher (10 mg/ml corresponding to $W_o = 0.82W_s$) than reported here (6.7 mg/ml corresponding to $W_o = 1.27W_s$). Regardless of the solubility figure used, the data of Ref. 16 plot well according to Eq. 7 (as shown in Fig. 7) and Eq. 5 (as shown in Fig. 8).

[2] Jacketed beaker, ACE Glass Corp., Vineland, N.J.

[3] LAB Vibrostatic pump, Lab Apparatus Co., Cleveland, OH 44128

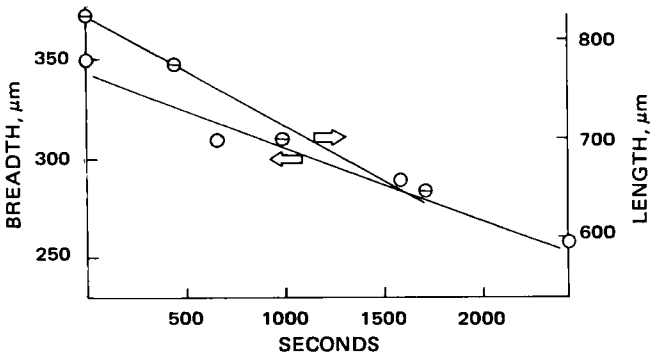

Figure 3—*Dissolution rate experiment conducted with single crystal of* p-*hydroxybenzoic acid in 0.1* N *HCl on microscope slide.*

converted to grams of *p*-hydroxybenzoic acid per 500 ml at the testing temperature by knowledge of the density of *p*-hydroxybenzoic acid solutions (at various concentrations) at the testing temperature. The results of these studies are shown in Fig. 2*a*. No more than five samples were removed during a test; if more points were necessary, the experiment was repeated at the different time points desired.

An experiment was also performed using an amount of *p*-hydroxybenzoic acid corresponding to 1.15 $W_s = W_o$, and an experiment was performed with a 16–20 sieve cut with 1.5 $W_s = W_o$. A dissolution rate experiment on a crystal of *p*-hydroxybenzoic acid was performed on a microscope slide in 3 drops of 0.1 *N* HCl by the method described by Carstensen and Patel (6); the length *(b)* and the breadth *(a)* decrease linearly in time as shown in Fig. 3.

A microscopic determination of the dimensions of 60 particles was performed (Fig. 4). *p*-Hydroxybenzoic acid is actually monoclinic, but the crystals approximate a rectangular parallelepiped with sides *a*, *a* and *b*; Fig. 4 shows that the ratio of *b* to *a* is about 2.4. Since, as seen in Fig. 3, the rate constant for the breadth is $k_a \sim 0.04$ cm/sec and the rate constant for the length is $k_b \sim 0.1$ cm/sec, $k_b/k_a \sim 2.5$, which is close to the ratio of the sides (= 2.4). Since, therefore, the sides decrease in magnitude with rates approximately proportional to the lengths themselves, the dissolution is considered fairly isotropic.

The volumes ($V = a^2b$) of the particles in Fig. 4 were calculated based on the assumption that the particles are parallelepipeds. The cube length equivalents ($\sqrt[3]{V}$) calculated in this fashion are shown in Table I. If the sieve cut were from a single crystallization, it would be expected to have a monotonely decreasing frequency function with increasing particle size (with the assumption that the sieve cut is above the number based mean). Since it is a blend of several batches, this, of course, cannot be expected. In fact, the distribution appears to be a square distribution (*i.e.*, frequency is equal for each size within the cut). The data in Table I fail to show a significant difference from such a distribution ($\chi^2 = 12$, which is smaller than the critical χ^2-value for 11 degrees of freedom and a

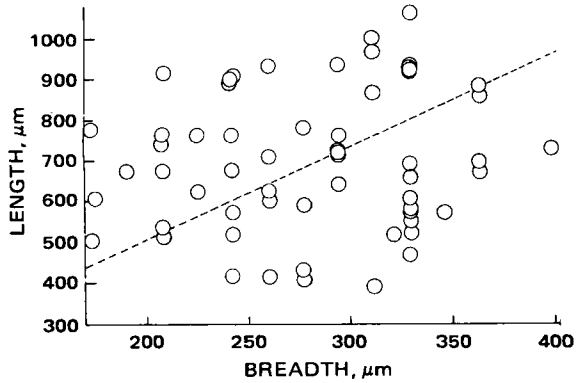

Figure 4—*Distribution of dimensions of 60 crystals of* p-*hydroxybenzoic acid of a 40–60 sieve cut.*

Table I—Distribution of Crystals from Fig. 4

10^{-3} $V^{1/3}$ Interval, μm	Logarithm of Lower Number	Number of Crystals in Interval	Percent Crystals (Cumulative)
1.1–1.2	0.041	2	3.3
1.2–1.3	0.079	2	6.3
1.3–1.4	0.114	5	14.6
1.4–1.5	0.146	9	29.6
1.5–1.6	0.176	4	36.3
1.6–1.7	0.204	5	44.6
1.7–1.8	0.230	8	57.9
1.8–1.9	0.255	8	71.2
1.9–2.0	0.279	2	74.5
2.0–2.1	0.301	5	82.8
2.1–2.2	0.322	6	92.8
2.2–2.3	—	4	100

probability of 0.05, $\chi^2_{crit} = 19.7$). Brooke (19) recently discussed this type of phenomenon in depth.

DISCUSSION

Although the data by Niebergall and Goyan (14) suggest that the negative two-thirds relation (Eq. 4) holds to 30% of saturation only, data from other literature sources suggest that it may have wider applicability. Figure 5 shows the data from Wilhelm *et al.* (9) for $W_o = W_s$; the test substance was sodium chloride, and the data adhere to Eq. 4 to better than 80%. Deviations above 80% are due to the fact that, in this range, the difference is a small difference between large numbers.

The data from the dissolution of *p*-hydroxybenzoic acid shown in Fig. 2*a* are shown plotted according to Eq. 4 in Fig. 2*b*. Here, again, the data adhere to Eq. 4 to better than 80% of solubility. The deviations from adherance to Eq. 4 are negative and are attributed to the fact that (aside from the poor precision in the higher range) the 40–60-mesh material is not quite monodisperse, so loss of the smallest particles occurs in this range.

As shown in the *Appendix* (Eq. A8), Eq. 4 can be written:

$$(W/W_o)^{-2/3} - 1 = S^{2/3}2kN^{1/3}\Gamma/(3V^{1/3})t = Bt \quad \text{(Eq. 9}a\text{)}$$

or:

$$(W/W_o)^{-2/3} - 1 = [4kS/(\rho d_o)]t \quad \text{(Eq. 9}b\text{)}$$

It follows that the slope, *B*, adheres to:

$$\ln (B/T) = \ln S + \ln (k/T) + \ln[4/(\rho d_o)] \quad \text{(Eq. 10)}$$

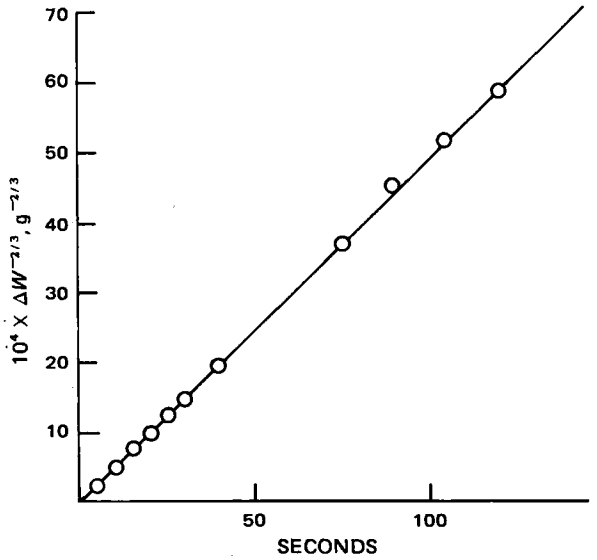

Figure 5—*Data from Ref. 9 plotted according to Eq. 4 when* $W_o = W_s$.

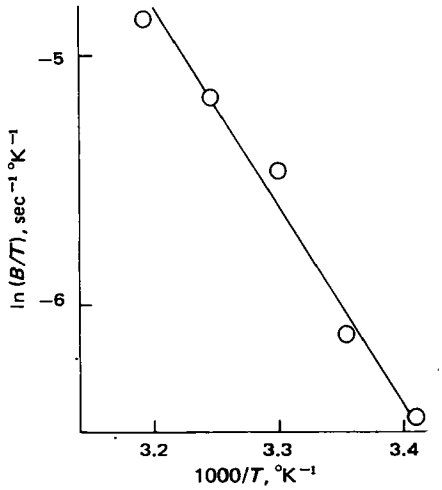

Figure 6—*The slopes,* B, *from Fig. 5 plotted as ln* (B/T) *as a function of reciprocal absolute temperature (1000/T °K^{-1}).*

Carstensen and Patel (6) showed that ln (k/T) is linear with $1/T$ with a slope of between E/R and $2E/R$, where E (<0) is the activation energy for the viscosity of the dissolution medium, and the $2E/R$ term holds with higher agitation intensities such as are reported here. The data in Fig. 1 give ln $S = [-(\Delta H/R)(1/T)] + q$, where ΔH is the heat of solution and q is a constant. From the data in Fig. 1, it is seen that $(\Delta H/R) = 4850$ cal/mole.

Therefore, a plot of ln (B/T) *versus* $1/T$ should be linear and have a slope of $[(2E/R) - \Delta H]$. The linearity is demonstrated in Fig. 6; the slope is −8000 cal/mole. Therefore, $(2E/R) - 4850 = -8000$; *i.e.*, E is between −3150 and −6300 cal/mole, close to E for water (−4700 cal/mole). An equation derived from the film theory (Eq. 4) apparently shows consistency in temperature dependence and the attained slopes are of the expected magnitude.

In spite of several assumptions in the film theory (*viz.*, isotropicity, isometricness, constant film thickness, neglect of convection, and size-independent solubility) and some experimental approximations (*viz.*, geometric surface areas and the assumption of well-defined particle size), the data developed from the theory adhere well to experimental values. This statement is not an attempt to minimize the theoretical importance of the assumptions but simply notes that the effects of the assumptions either cancel out or fall below experimental scrutiny in many cases.

Other equations (15, 16) are also based on simple film theory with the same assumptions. They basically do not differ, and it is apparent from the *Appendix* that data following one should also follow the other. Literature data (9, 16) are shown plotted according to Eq. 7 in Fig. 7 and according to Eq. 5 in Fig. 8, and the data hold up to about 70% of saturation.

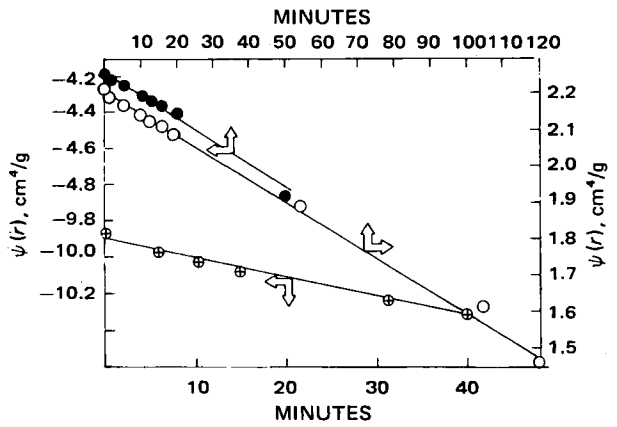

Figure 7—*Data plotted according to Eq. 7. Key:* ⊕, *data from Ref. 9 where initial weight* $W_o = 1.2W_s$; ○, *data from Ref. 16 where initial weight* $W_o = 0.82W_s$; *and* ●, *data from Ref. 16 where initial weight* $W_o = 1.27W_s$.

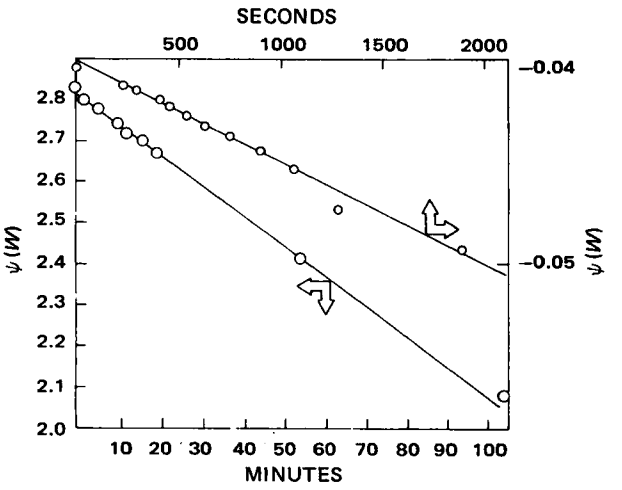

Figure 8—*Data plotted according to Eq. 5. Key:* ○, *sodium chloride data from Ref. 9 where initial weight* $W_o = 1.2W_s$; *and* ○, p-*hydroxybenzoic acid data from Ref. 16 where initial weight* $W_o = 0.82W_s$.

The derivations of Eqs. 5 and 7 require that $W_o < W_s$ or $W_s < W_o$. A dissolution test using p-hydroxybenzoic acid at $W_o = 1.15W_s$ is shown in Fig. 9, and the data, again, adhere to both Eqs. 7 and 5 to about 70% of saturation. In all cases, the deviation is in the direction of smaller k values. Neither the concept that film thickness decreases with the size of the particle nor the concept that solubility increases with a decrease in particle size would explain this result, since the former, in decreasing h, would *increase* k $(=D/h)$ and the latter would increase the concentration gradient and, hence, the dissolution rate. It may, however, be fallacious to consider a sieve fraction comparable to monodisperse powder.

The point here is that, essentially, one is equating the surface area of the "mean" particle size with the surface area of the sieve cut. If particles were isotropic, then the most proper mean to use would be of the volume–surface type; using the cube length equivalent, it is possible to define $\bar{x}_{sv} = \Sigma nx^3/(\Sigma nx^2) = [\int f(x)x^3\,dx]/[\int f(x)x^2\,dx]$, where $f(x)$ is the frequency of the occurrence of the length x. However, the use of the number average mean here gives better results from a surface area point of view.

If one considers the data in Table I as representing a square distribution, then the frequency function, $f(x)$, would be independent of particle length, *i.e.*:

$$f(x) = A \qquad \text{(Eq. 11)}$$

where A is a constant. Normalizing this over the interval of 110–230 μm yields:

$$\int_{110}^{230} f(x)\,dx = 120A = 1 \qquad \text{(Eq. 12}a\text{)}$$

so that:

$$A = 1/120\ (\mu m)^{-1} \qquad \text{(Eq. 12}b\text{)}$$

The surface area (per one particle equivalent) of a sieve fraction

Table II—Errors in Assuming a Sieve Cut of 40–60 Mesh to be Monodisperse Assuming Linear Length Reduction during Dissolution

x_1, μm	x_2, μm	$\bar{x}$, μm	A/A^*	Percent Dissolved	Volume[a], μm^3
110	230	170	1.04	0	$5.5\ 10^6$
80	200	140	1.06	43	$3.23\ 10^6$
55	175	115	1.09	65	$1.93\ 10^6$
20	140	80	1.19	85	$0.80\ 10^6$
0	120	60	1.33	97	$0.24\ 10^6$

[a] Normalized to the equivalent of one particle.

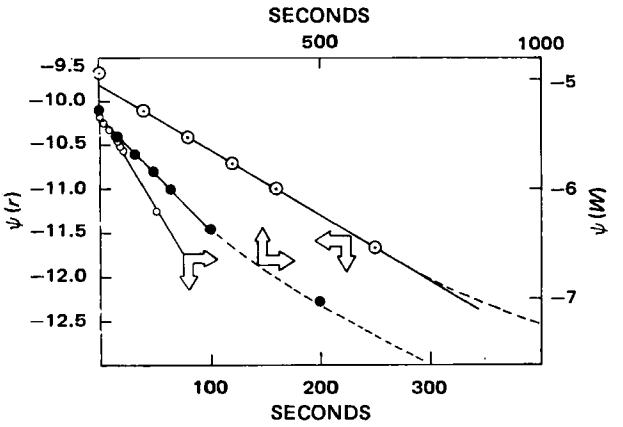

Figure 9—*Data from this study plotted according to Eqs. 5 and 7. Key:* ⊙, *p-hydroxybenzoic acid at 25°, 40–60 mesh, using Eq. 7 with initial weight* $W_o = 1.15W_s$; ●, *p-hydroxybenzoic acid at 25°, 40–60 mesh, using Eq. 5 with initial weight* $W_o = 1.15W_s$; *and* ○, *p-hydroxybenzoic acid at 25°, using Eq. 7 with initial weight* $W_o = 1.27W_s$ *from Ref. 16.*

between x_1 μm and x_2 μm is given by:

$$A = (1/120)\int_{x_1}^{x_2} 6x^2\,dx = (1/60)\,(x_2^3 - x_1^3) \quad \text{(Eq. 13)}$$

The volume (per one particle equivalent) of a sieve fraction between x_1 μm and x_2 μm is given by:

$$A = (1/120)\int_{x_1}^{x_2} x^3\,dx = (1/480)\,(x_2^4 - x_1^4) \quad \text{(Eq. 14)}$$

If one assumes that x_1 decreases at the same rate as x_2, then one can calculate the area of the sieve fraction A as opposed to the area (A^*) it would have had if it had been monodisperse with the arithmetic mean diameter. Data computed in this fashion are shown in Table II. The area estimate is relatively close up to about 65% dissolved, at which point it is 10% high. The A/A^* increases (almost linearly) up to 65% dissolved, after which it rises drastically; this increase would impart linearity to plots *via* Eq. 5 or 7, but the slopes would differ somewhat from those given by the equations.

It is noted that $x_{sv} = 138$ μm; if this value (rather than 170 μm) had been used in Table II, deviations would have been greater. (This would not be so for example with a true sphere.) The assumption that x_1 and x_2 decrease with the same rate is not correct, and actual figures would be less favorable than those shown in Table II.

In a semiquantitative way, the foregoing arguments imply that,

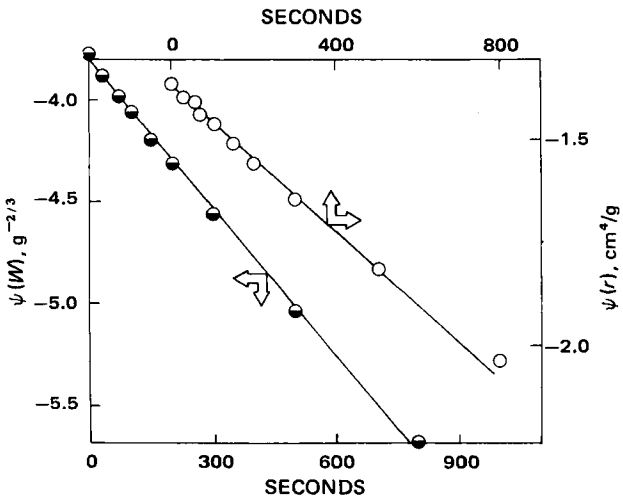

Figure 10—*Data from this study plotted according to Eq. 5 (⊖) and Eq. 7 (○) with p-hydroxybenzoic acid at 25°, 16–20 mesh, and initial weight* $W_o = 1.5W_s$.

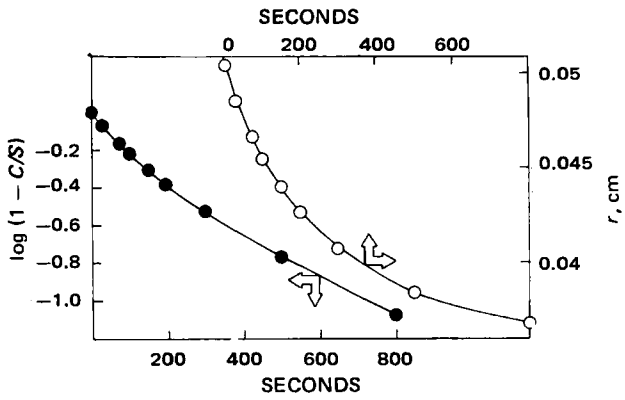

Figure 11—*Data from Fig. 10 plotted (●) according to Eq. 15 (which assumes constant surface area). Curve to the right (○) shows the change in radius (assuming spherical particles) as a function of time.*

in the case of the 40–60 cut, adherance to predicted equations could be expected to only about 65% of complete dissolution of the available solid when $W_o < W_s$ (and to more than 65% of the complete dissolution process when $W_o > W_s$). In Figs. 2*b* and 7–9, linearity prevails to better than 70% of complete dissolution or of the dissolution process; the use of sieve cuts apparently is an explanation for nonadherance beyond this point. The relatively larger A value has the effect of a larger r value in Eq. 7, which gives a higher value of $\psi(r)$ (smaller value of k). This trend is shown in Fig. 9.

Higher W_o's and larger particle sizes should reduce these effects, and the data in Fig. 10 ($W_o = 1.5W_s$, 16–20-mesh fraction) show that this coarser sample in higher amounts adheres to Eqs. 5 and 7 through the whole dissolution process. At very high amounts of material used, the point will be reached where the surface area will stay practically constant during the dissolution process and should follow (11):

$$\ln[1 - (C/S)] = -kOt/V \quad \text{(Eq. 15)}$$

It is seen from Fig. 11 that $W_o = 1.5W_s$ is not a sufficiently large excess of powder to make Eq. 15 apply. Larger excesses are difficult to test, since dissolution becomes rapid with the increased surface areas.

A secondary observation makes the previous considerations pertinent to many actual samples of recrystallized powders. Many crystallizers are built on the principle of nonisothermal crystallization followed by fines destruction (through a raise in temperature at the end of the process). Blending of batches is also a practice, and it would, therefore, be expected that distributions other than log normal would result and that distributions such as the one shown in Table I might be common. As shown in Fig. 12, a cumulative plotting of this type resembles a log-normal distribution, and this may be one reason (other than the reasons stated in the literature) that crystallized materials appear to be log normal.

In conclusion, it should be mentioned once again that a series of

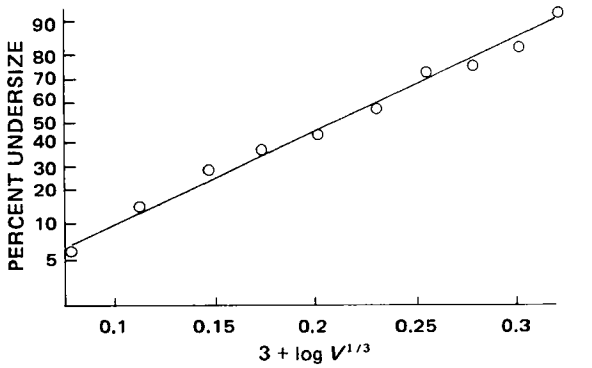

Figure 12—*Data from Fig. 4 shown as a log-normal distribution.*

assumptions is made in the basic film theory of dissolution which cannot be disregarded in dissolution work. However, in studying dissolution behaviors of powder samples, experimental techniques at present do not suffice to detect the effect of the assumptions because of the difficulty in producing monodisperse samples of crystalline samples. In general, film theory has produced equations through a large range of W_o values [Eqs. 5 and 7, Eq. 2 (the cube root law), Eq. 4 (the negative two-thirds law), and Eq. 15], which are workable models for dissolution of powders.

APPENDIX

The Noyes–Whitney equation (1) in the nomenclature used here is:

$$-dW/dt = kO(S - C) \qquad \text{(Eq. A1)}$$

where O is surface area at time t. The concentration, C, may be expressed as $(W_o - W)/V$, and saturation concentration, S, may be expressed as W_s/V, so that Eq. A1 becomes:

$$-V(dW/dt) = kO[W_s - (W_o - W)] \qquad \text{(Eq. A2)}$$

For N particles, the surface area and weights are given by:

$$O = N\pi d^2 \qquad \text{(Eq. A3)}$$

$$W = N\pi d^3\rho/6 \qquad \text{(Eq. A4)}$$

so that:

$$OW^{-2/3} = N^{1/3}[6/(\pi\rho)]^{2/3}\pi = N^{1/3}[6\sqrt{\pi}/\rho]^{2/3} = N^{1/3}\Gamma \qquad \text{(Eq. A5)}$$

Inserting Eq. A5 in Eq. A2 then gives:

$$-V(dW/dt) = kN^{1/3}\Gamma W^{2/3}[W_s - W_o + W] \qquad \text{(Eq. A6)}$$

If $W_s = W_o$, then this becomes:

$$-dW/(W^{5/3}) = (kN^{1/3}\Gamma/V)\,dt \qquad \text{(Eq. A7)}$$

which can be integrated and subjected to initial conditions to give:

$$W^{-2/3} - W_o^{-2/3} = \frac{2kN^{1/3}\Gamma}{3V}t \qquad \text{(Eq. A8)}$$

which is equivalent to the Niebergall equation (Eq. 4).

In general, Eq. A6 can be simplified by introduction of the following substitutions:

$$W_s - W_o = F^3 \qquad \text{(Eq. A9)}$$

$$W = u^3 \qquad \text{(Eq. A10)}$$

in which case it becomes:

$$du/(F^3 + u^3) = (kN^{1/3}\Gamma/3V)dt \qquad \text{(Eq. A11)}$$

which, after integration and use of initial conditions, gives the Short–Sharkey–Rhodes equation (Eq. 5)[4].

REFERENCES

(1) A. A. Noyes and W. R. Whitney, *J. Amer. Chem. Soc.*, **19,** 930(1897).

(2) W. Nernst, *Z. Phys. Chem. (Leipzig)*, **47,** 52(1904).

(3) E. Brunner, *ibid.*, **47,** 56(1904).

(4) M. L. Brunner and St. Tolloczko, *Z. Anorg. Allgem. Chem.*, **28,** 314(1901); *ibid.*, **35,** 23(1903); *ibid.*, **56,** 58(1907).

(5) P. J. Niebergall, G. Milosovich, and J. E. Goyan, *J. Pharm. Sci.*, **52,** 236(1963).

(6) J. T. Carstensen and M. Patel, *J. Pharm. Sci.*, in press.

(7) W. Ostwald, *Z. Phys. Chem.*, **22,** 289(1897).

(8) H. Freundlich, "Colloid and Capillary Chemistry," E. P. Dutton, New York, N.Y., 1922, p. 122.

(9) R. H. Wilhelm, L. H. Conklin, and T. C. Sauer, *Ind. Eng. Chem.*, **33,** 453(1941).

(10) A. W. Hixson and J. H. Crowell, *ibid.*, **23,** 923(1931).

(11) J. T. Carstensen, in "Dissolution Technology," L. Leeson and J. T. Carstensen, Eds., Industrial Pharmaceutical Technology, APhA Academy of Pharmaceutical Sciences, Washington, D.C., 1974.

(12) W. Jost, "Diffusion," Academic, New York, N.Y., 1960, p. 140.

(13) C. R. Wilke, *Chem. Eng. Progr.*, **54** (3), 218(1949).

(14) P. J. Niebergall and J. E. Goyan, *J. Pharm. Sci.*, **52,** 29(1963).

(15) M. P. Short, P. Sharkey, and C. T. Rhodes, *ibid.*, **61,** 1733(1972).

(16) P. Pothisiri and J. T. Carstensen, *ibid.*, **62,** 1468(1973).

(17) K. G. Nelson and A. C. Shah, "Abstracts of the APhA Academy of Pharmaceutical Sciences," Washington, D.C., paper 70, 1974.

(18) A. C. Shah and K. G. Nelson, *ibid.*, paper 71, 1974.

(19) D. Brooke, *J. Pharm. Sci.*, **64,** 1409(1975).

ACKNOWLEDGMENTS AND ADDRESSES

Received December 2, 1974, from the *School of Pharmacy, University of Wisconsin, Madison WI 53706*

Accepted for publication February 19, 1975.

The authors are indebted to Mr. R. Sowinski and Mr. Thomas Lai for assistance.

[x] To whom inquiries should be directed.

[4] The equation differs slightly from that reported by Short *et al.* (15) due to a printing error in Ref. 15.